



**HAL**  
open science

## **CYLD Regulates Centriolar Satellites Proteostasis by Counteracting the E3 Ligase MIB1**

Tiphaine Douanne, Gwennan André-Grégoire, An Thys, Kilian Trillet, Julie Gavard, Nicolas Bidère

► **To cite this version:**

Tiphaine Douanne, Gwennan André-Grégoire, An Thys, Kilian Trillet, Julie Gavard, et al.. CYLD Regulates Centriolar Satellites Proteostasis by Counteracting the E3 Ligase MIB1. Cell Reports, 2019, 27 (6), pp.1657-1665. 10.1016/j.celrep.2019.04.036 . inserm-02128157

**HAL Id: inserm-02128157**

**<https://inserm.hal.science/inserm-02128157v1>**

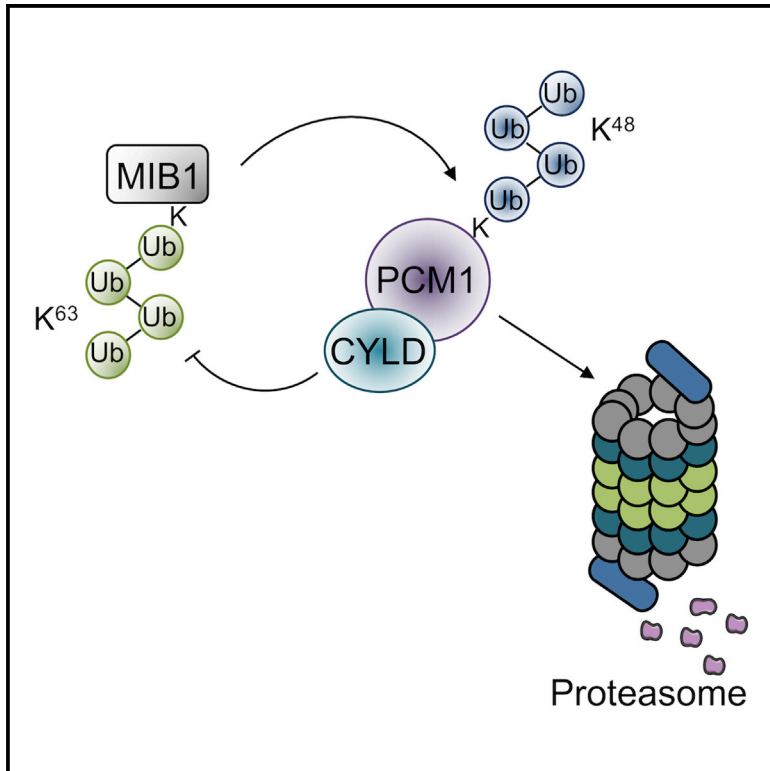
Submitted on 14 May 2019

**HAL** is a multi-disciplinary open access archive for the deposit and dissemination of scientific research documents, whether they are published or not. The documents may come from teaching and research institutions in France or abroad, or from public or private research centers.

L'archive ouverte pluridisciplinaire **HAL**, est destinée au dépôt et à la diffusion de documents scientifiques de niveau recherche, publiés ou non, émanant des établissements d'enseignement et de recherche français ou étrangers, des laboratoires publics ou privés.

## CYLD Regulates Centriolar Satellites Proteostasis by Counteracting the E3 Ligase MIB1

### Graphical Abstract



### Authors

Tiphaine Douanne,  
Gwennan André-Grégoire, An Thys,  
Kilian Trillet, Julie Gavard, Nicolas Bidère

### Correspondence

nicolas.bidere@inserm.fr

### In Brief

Douanne et al. find that a subset of the deubiquitinating enzyme CYLD is part of the centriolar satellites and controls their proteostasis, therefore allowing the formation of primary cilia. They show that CYLD removes ubiquitin from the E3 ligase MIB1 and prevents MIB1-mediated dismantlement of centriolar satellites.

### Highlights

- A subset of CYLD is found at the centriolar satellites
- CYLD maintains the proteostasis of the centriolar satellites
- CYLD removes ubiquitin chains bound to the E3 ligase MIB1
- CYLD counteracts MIB1-mediated disruption of the centriolar satellites



# CYLD Regulates Centriolar Satellites Proteostasis by Counteracting the E3 Ligase MIB1

Tiphaine Douanne,<sup>1</sup> Gwennan André-Grégoire,<sup>1,2</sup> An Thys,<sup>1</sup> Kilian Trillet,<sup>1</sup> Julie Gavard,<sup>1,2</sup> and Nicolas Bidère<sup>1,3,\*</sup><sup>1</sup>CRCINA, Team SOAP, INSERM, CNRS, Université de Nantes, Université d'Angers, IRS-UN blg, Room 405, 8 quai Moncousu, 44007 Nantes, France<sup>2</sup>Institut de Cancérologie de l'Ouest, Site René Gauducheau, Saint-Herblain, France<sup>3</sup>Lead Contact\*Correspondence: [nicolas.bidere@inserm.fr](mailto:nicolas.bidere@inserm.fr)<https://doi.org/10.1016/j.celrep.2019.04.036>

## SUMMARY

The tumor suppressor CYLD is a deubiquitinating enzyme that removes non-degradative ubiquitin linkages bound to a variety of signal transduction adaptors. CYLD participates in the formation of primary cilia, a microtubule-based structure that protrudes from the cell body to act as a “sensing antenna.” Yet, how exactly CYLD regulates ciliogenesis is not fully understood. Here, we conducted an unbiased proteomic screen of CYLD binding partners and identified components of the centriolar satellites. These small granular structures, tethered to the scaffold protein pericentriolar matrix protein 1 (PCM1), gravitate toward the centrosome and orchestrate ciliogenesis. CYLD knockdown promotes PCM1 degradation and the subsequent dismantling of the centriolar satellites. We found that CYLD marshals the centriolar satellites by deubiquitinating and preventing the E3 ligase Mindbomb 1 (MIB1) from marking PCM1 for proteasomal degradation. These results link CYLD to the regulation of centriolar satellites proteostasis and provide insight into how reversible ubiquitination finely tunes ciliogenesis.

## INTRODUCTION

Ubiquitination is a pivotal post-translational modification involved in numerous cellular processes in eukaryotes (Komander and Rape, 2012). It consists of the covalent ligation of ubiquitin as a single moiety or as chains onto substrate proteins. The topology of ubiquitin modifications alters the substrates' interactome and leads to different cellular outcomes. These include targeting for proteasomal degradation, modulating protein activity, and promoting protein-protein interactions. Ubiquitination is a versatile process and is reversed by a family of proteases named deubiquitinating enzymes (DUBs), which selectively trim ubiquitin from their substrates (Mevisen and Komander, 2017).

The DUB cylindromatosis (CYLD) is a bona fide tumor suppressor that contains three NH<sub>2</sub>-terminal cytoskeleton associated protein glycine-rich (CAP-Gly) domains allowing microtubule binding. In addition, CYLD contains a COOH-terminal catalytic ubiquitin specific protease (USP) domain (Yang and Zhou,

2016). CYLD specifically hydrolyses Lys<sup>63</sup> (K<sup>63</sup>) and linear Met<sup>1</sup> (M<sup>1</sup>) ubiquitin linkages bound to a variety of signal transduction elements and therefore regulates a plethora of signaling pathways (Hrdinka and Gyrd-Hansen, 2017). For instance, CYLD regulates some NF- $\kappa$ B signaling pathways and cell death by necroptosis together with its recently identified binding partner spermatogenesis-associated protein 2 (SPATA2) (Elliott et al., 2016; Kupka et al., 2016; Schlicher et al., 2016; Wagner et al., 2016). CYLD has also been linked to ciliogenesis (Yang and Zhou, 2016). Cilia are microtubule-based structures that protrude from the cell body and act as a “sensing antenna” to detect and integrate various extracellular signals (Malicki and Johnson, 2017). *Cyld* knockout mice or transgenic mice carrying truncated catalytically dead CYLD exhibit defects in cilia formation in multiple organs and display several symptoms reminiscent of ciliopathies, a wide set of human syndromes caused by mutations in genes involved in ciliogenesis (Eguether et al., 2014; Jin et al., 2008; Trompouki et al., 2009; Wright et al., 2007; Yang et al., 2014).

How exactly CYLD participates in ciliogenesis continues to be elucidated. For instance, CYLD was shown to bind the centrosomal proteins CAP350, CEP192, and CEP70, and both its catalytic activity and its first two NH<sub>2</sub>-terminal CAP-Gly domains enable ciliogenesis (Eguether et al., 2014; Gomez-Ferrera et al., 2012; Yang et al., 2014). CYLD also binds and inactivates the histone deacetylase 6 (HDAC6), therefore driving tubulin acetylation and primary cilia formation (Yang et al., 2014). Here, combining an unbiased proteomic screen with confocal microscopy and biochemistry, we report that a subset of CYLD locates and interacts with centriolar satellites. Centriolar satellites are small non-membranous granules, tethered to the scaffold pericentriolar material 1 (PCM1), that cluster around the centrosome in a microtubule-dependent way. Emerging evidence has highlighted that centriolar satellites are involved in centrosome assembly and function and orchestrate ciliogenesis (Dammernann and Merdes, 2002). Mutations in some genes encoding for centriolar satellites components lead to defects in primary cilia and cause ciliopathies (Hori and Toda, 2017). Recently, the E3 ligase Mindbomb1 (MIB1) was proposed to disassemble the centriolar satellites and suppress ciliogenesis by marking PCM1 for proteasomal degradation (Lecland and Merdes, 2018; Wang et al., 2016). How PCM1 counteracts MIB1 to maintain centriolar satellites is unknown. We now describe how CYLD marshals the centriolar satellites by deubiquitinating MIB1, therefore preventing MIB1 from eliminating PCM1.



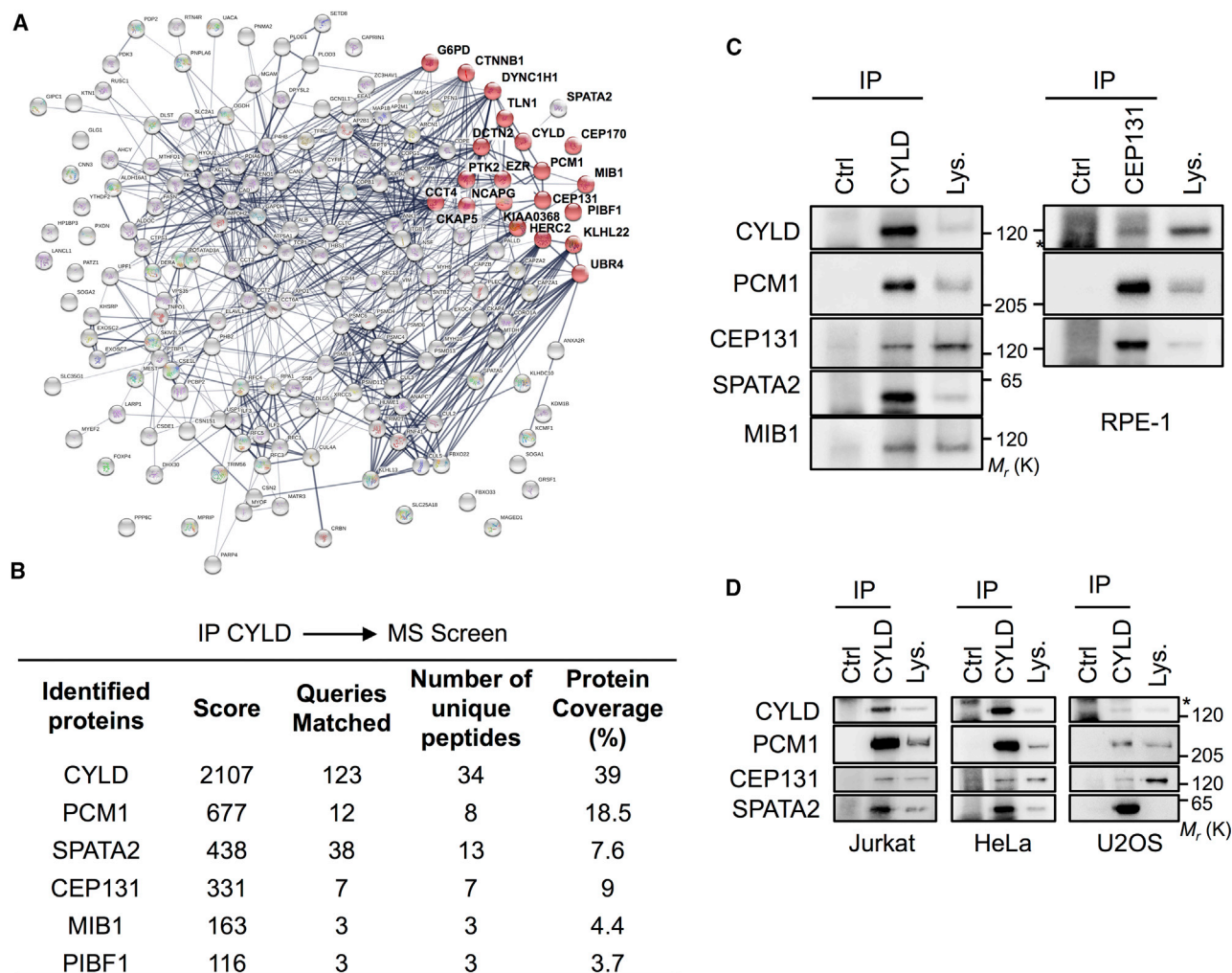


**Figure 1. Proteomic Analysis of CYLD Interactome Identifies Centriolar Satellites Components**

(A) Mass spectrometry (MS) analysis of immunoprecipitates (IP) prepared from RPE-1 cell lysates with antibodies specific for CYLD. Shown is a STRING analysis of 229 proteins found in the IP with microtubule organizing center proteins highlighted in red.

(B) MS-identified centriolar satellites elements derived from the IP. The protein score is the sum of the unique peptide score calculated following  $-10\log(P)$ , where  $p$  is 0.05. “Queries Matched” corresponds to the number of MS/MS identified for said protein; the numbers of unique peptide and protein coverage are shown.

(C and D) Cell lysates (Lys.) prepared from RPE-1 (C) and U2OS, Jurkat, and HeLa (D) cells were subjected to IP with antibodies against the indicated proteins, and samples were then analyzed by immunoblotting as indicated. Ctrl represents the nonrelevant isotype-matched antibodies. Asterisks (\*) indicate non-specific bands. Molecular weight markers are shown. Data are representative of three independent experiments.

## RESULTS AND DISCUSSION

### CYLD Interacts with Components of the Centriolar Satellites

To uncover novel effectors of CYLD functions, we conducted an unbiased mass spectrometry screen in retinal-pigmented epithelial (RPE-1) cells. As expected (Elliott et al., 2016; Kupka et al., 2016; Schlicher et al., 2016; Wagner et al., 2016), SPATA2 was found as a binding partner. The identified hits were further processed using the STRING public online database (<https://string-db.org>), which sorts functional interactions between proteins. Performing a Gene Ontology (GO) analysis unveiled a cluster of microtubule-organizing center (mTOC) elements (Figure 1A). Among those, four elements of the centriolar satellites

(PCM1, CEP131, MIB1, and PIBF1) were isolated (Figure 1B). Centriolar satellites are small granules that gravitate toward the centrosome in a microtubule-dependent way and coordinate cillogenesis (Hori and Toda, 2017). Within the centriolar satellites, PCM1 associates to most proteins and is therefore thought to scaffold those structures (Hori and Toda, 2017). Co-immunoprecipitation experiments confirmed that CYLD bound to the centriolar satellites resident proteins PCM1, CEP131, and MIB1 in cells of diverse lineages (Figures 1C, 1D, S1A, and S1B). Likewise, CEP131 pull-down also precipitated CYLD (Figure 1C). Although known partners of CYLD at the centrosome were absent from our mass spectrometry analysis, the centrosome marker  $\gamma$ Tubulin efficiently co-immunoprecipitated with CYLD (Figure S1C). Taken together, our data suggest that

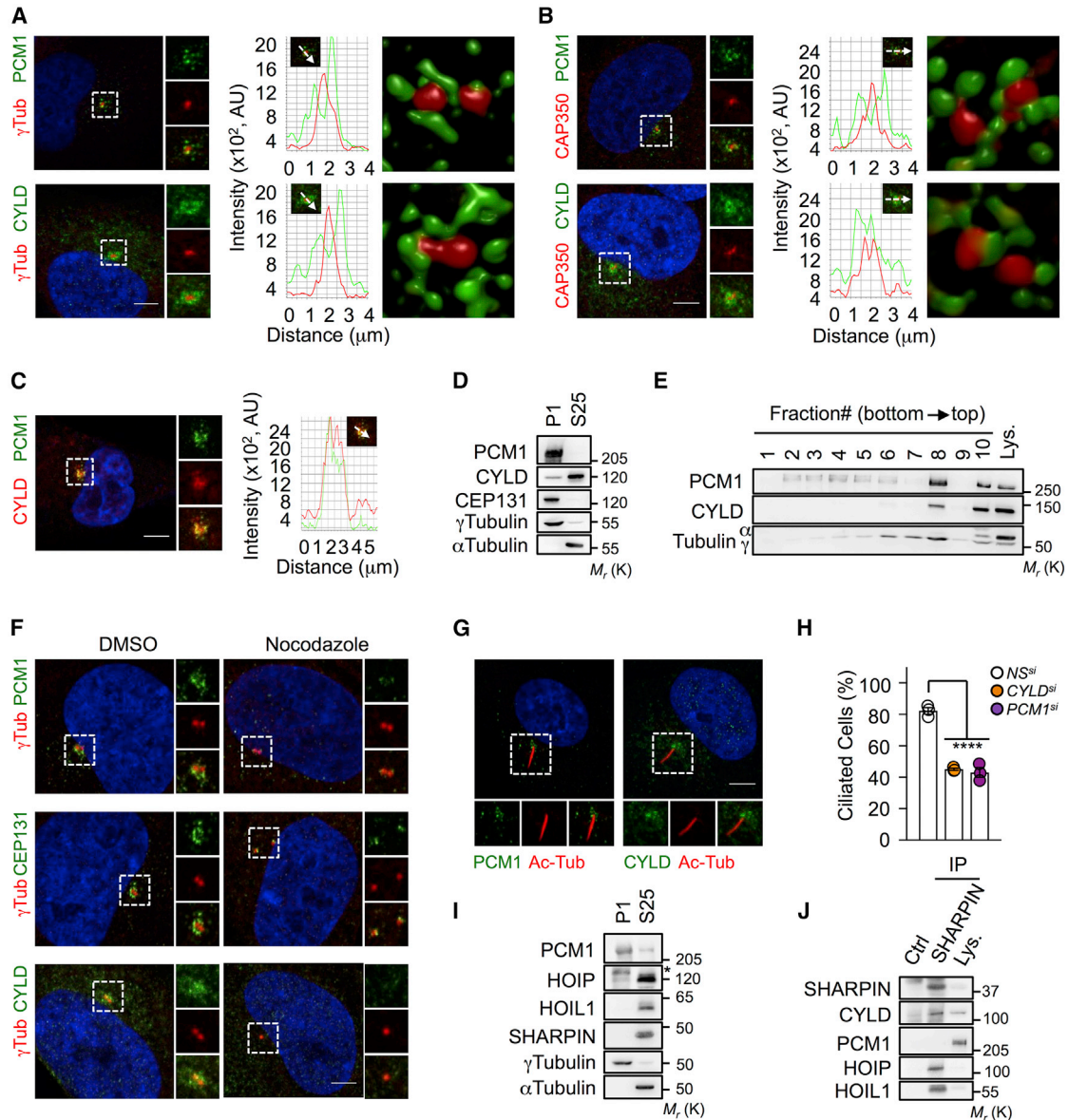


**Figure 2. CYLD Is a Component of Centriolar Satellites**

(A and B) Confocal microscopic analysis of RPE-1 cells showing the localization of the centrosome resident proteins  $\gamma$ Tubulin ( $\gamma$ Tub) (A) or CAP350 (B) together with PCM1 or CYLD, with nuclei stained by 4', 6-diamidino-2-phenylindole (DAPI). Regions highlighted by white squares are shown under higher magnification in panels on the right. AU represents arbitrary units. Scale bar, 5  $\mu$ m. Data are representative of three independent experiments. The middle panels are a quantification of staining intensity alongside the white arrow. The left panels show the staining analysis by structure illumination microscopy (SIM).

(C) RPE-1 cells overexpressing PCM1-GFP were analyzed by confocal microscopy as in (A). Scale bar, 5  $\mu$ m. Quantification of staining intensity alongside the white arrow is shown. Data are representative of two independent experiments.

(D) Subcellular fractionation of RPE-1 cell to yield a P1 fraction enriched with centriolar satellites and centrosomes, and a S25 fraction enriched with cytosolic proteins. Samples were analyzed by immunoblotting as indicated. Data are representative of three independent experiments.

(E) Lys. from RPE-1 cells were fractionated on discontinuous sucrose gradients (10%–50%). Ten fractions were collected and analyzed by immunoblotting as indicated. Shown is an experiment representative of three independent experiments.

(F) Confocal microscopy analysis of RPE-1 cells treated with 2  $\mu$ g.mL<sup>-1</sup> of nocodazole or vehicle DMSO for 2 h. Data are representative of three independent experiments.

(G and H) RPE-1 cells were transfected with small interfering RNA (siRNA) for CYLD, PCM1 or scramble non-specific (NS) siRNA for 48 h, and serum-starved for 24 h to induce ciliogenesis. Confocal micrographs are shown. Acetylated tubulin (Ac-Tub) is used to visualize primary cilia. Scale bar, 5  $\mu$ m (G). Histogram showing quantification of ciliated cells (H); n > 100 per sample in three independent experiments (means  $\pm$  SEM; \*\*p < 0.01 [ANOVA]).

(legend continued on next page)

CYLD physically interacts with centriolar satellites and centrosomal components.

### CYLD Localizes in the Vicinity of Centriolar Satellites

We next compared the distribution of CYLD to that of the centrosomal resident proteins  $\gamma$ Tubulin and CAP350 by confocal microscopy. Like PCM1, CYLD staining revealed punctuate structures that formed a ring-shaped staining surrounding the centrosomes, consistent with a centriolar satellites localization (Figures 2A, 2B, S2A, and S2B). To more directly test PCM1 and CYLD proximity, CYLD was stained in RPE-1 cells overexpressing PCM1-GFP (Hori et al., 2016). Although CYLD was not exclusively at the centriolar satellites, CYLD and PCM1 co-localized (Figure 2C). Of note, CYLD binding partner SPATA2 displayed a similar distribution and bound to the centriolar satellites element CEP131 (Figures S2C–S2G). We further developed a cellular fractionation procedure to enrich centriolar satellites and centrosomes (P1 fraction) and noted the presence of CYLD alongside PCM1, CEP131, and  $\gamma$ Tubulin (Figure 2D). CYLD also coalesced with  $\gamma$ Tubulin and PCM1 when cell extracts were fractionated (Figure 2E). Centriolar satellites are efficiently disrupted during mitosis or in cells treated with the microtubule poison nocodazole (Dammermann and Merdes, 2002). Accordingly, PCM1 staining at the centriolar satellites was lost, whereas CEP131 relocalized to the centrosome (Figure 2F). We found that CYLD staining was dispersed in cells treated with nocodazole. Taken together, these data suggest that CYLD partially resides at the centriolar satellites.

Given the crucial role played by centriolar satellites in ciliogenesis (Hori and Toda, 2017), we first tracked CYLD during this process. Paralleling PCM1, CYLD accumulated at the base of the primary cilia in serum-starved RPE-1 cells (Figure 2G). Supporting a previous report (Yang et al., 2014), silencing of CYLD mRNA markedly decreased starvation-induced ciliogenesis, as did the knockdown of PCM1 (Figure 2H). Because part of CYLD interacts with the linear ubiquitination assembly complex (LUBAC) via SPATA2 (Elliott et al., 2016), we next evaluate the presence of this complex in centriolar satellites- and centrosome-enriched fractions. However, the core components of the LUBAC, namely, HOIP, HOIL1, and SHARPIN, merely accumulated in cytosolic fractions (Figure 2I). In keeping with this, pulling down the LUBAC using an antibody against SHARPIN showed an interaction with CYLD but not with PCM1 (Figure 2J). Taken together, our data suggest that CYLD segregates in independent exclusive complexes in cells, with a subset linked with the centriolar satellites and involved in ciliogenesis.

### CYLD Governs the Proteostasis of Centriolar Satellites

To investigate the impact of CYLD on the centriolar satellites, we next decreased its expression levels by RNA interference. In CYLD-silenced RPE-1 cells, PCM1 staining surrounding the centrosome was lost (Figures 3A and S3A). Further supporting a disruption of the centriolar satellites (Tollenaere et al., 2015),

CEP131 relocalized at the centrosome. Strikingly, the abundance of PCM1 and CEP131 was significantly reduced without CYLD, as assessed by immunoblot in RPE-1 and HeLa cells (Figures 3B, 3C, S3B, and S3C). No relocation of PCM1 into the cytosol was observed, suggesting degradation (Figure S3D). Although CEP131 proteostasis required PCM1, the opposite was not true, suggesting that the diminished levels of CEP131 may result from PCM1 elimination (Figure 3D). Of note, no overt change in PCM1 mRNA levels was observed (Figure 3E). We further found that this decrease in PCM1 and CEP131 abundance was partly reversed by a treatment with MG132 and Bortezomib, suggesting elimination of these centriolar satellites components by the proteasome (Figures 3F and S3E). Hence, CYLD may control the centriolar satellites proteostasis by preventing the proteasomal degradation of PCM1.

### CYLD Directly Deubiquitinates the Centriolar Satellites Gatekeeper MIB1

In sharp contrast to the disappearance of PCM1 and CEP131, we observed increased levels of the E3 ligase MIB1 in CYLD-silenced cells (Figures 4A, S4A, and S4B). However, CYLD knockdown had a minimal impact on MIB1 translation, suggesting a post-translational modification (Figure 4B). MIB1 was identified as an integral component of the centriolar satellites negatively regulating ciliogenesis and capable of decorating PCM1 and CEP131 with ubiquitin (Lecland and Merdes, 2018; Villumsen et al., 2013; Wang et al., 2016). When overexpressed in HEK293T, MIB1, and not catalytically dead MIB1, also underwent polyubiquitination, suggesting auto-ubiquitination (Wang et al., 2016; Figure S4C). Wang et al. (2016) further showed that overexpression of MIB1 promoted the polyubiquitination of PCM1 and CEP131 and their subsequent elimination. Accordingly, PCM1 abundance was increased in MIB1-silenced cells (Figure S4D). In return, PCM1 sequesters MIB1 to the centriolar satellites and maintains its level low through a yet-to-be-defined mechanism (Wang et al., 2016). Because CYLD associated with MIB1 in a PCM1-dependent manner (Figures 4C and S4E), we inferred that CYLD might temper MIB1 ubiquitination and MIB1-mediated centriolar satellites dismantling. We first used tandem ubiquitin binding entity (TUBE) to selectively pull down endogenous proteins marked with ubiquitin (Hjerpe et al., 2009). This revealed a significant increase in MIB1 ubiquitination when CYLD was silenced (Figure 4D). Importantly, ubiquitinated MIB1 was selectively pulled down with TUBE specific for K<sup>63</sup>, and not K<sup>48</sup>, linkages (Figure 4D), suggesting that MIB1 undergoes K<sup>63</sup> ubiquitination without CYLD. Accordingly, MIB1 ubiquitination was also visible in HEK293T cells co-transfected with MIB1 and a K<sup>63</sup>-only ubiquitin mutant and with a K<sup>48</sup>-only mutant to a lesser extent (Figure 4E).

Furthermore, ubiquitin attached to endogenous MIB1 in CYLD-silenced cells was efficiently removed with recombinant CYLD in a standard *in vitro* DUB assay (Figure 4F). The same was true with ectopically expressed MIB1 (Figure 4G), consistent

(I) Samples as in (D) were analyzed by immunoblotting. The asterisk (\*) indicates an NS band. The presented data are representative of at least three independent experiments.

(J) IPs were prepared from RPE-1 cell Lys. and analyzed by immunoblotting as indicated. Ctrl represents the control irrelevant isotype-matched antibodies. Molecular weight markers are shown. Data are representative of three independent experiments.

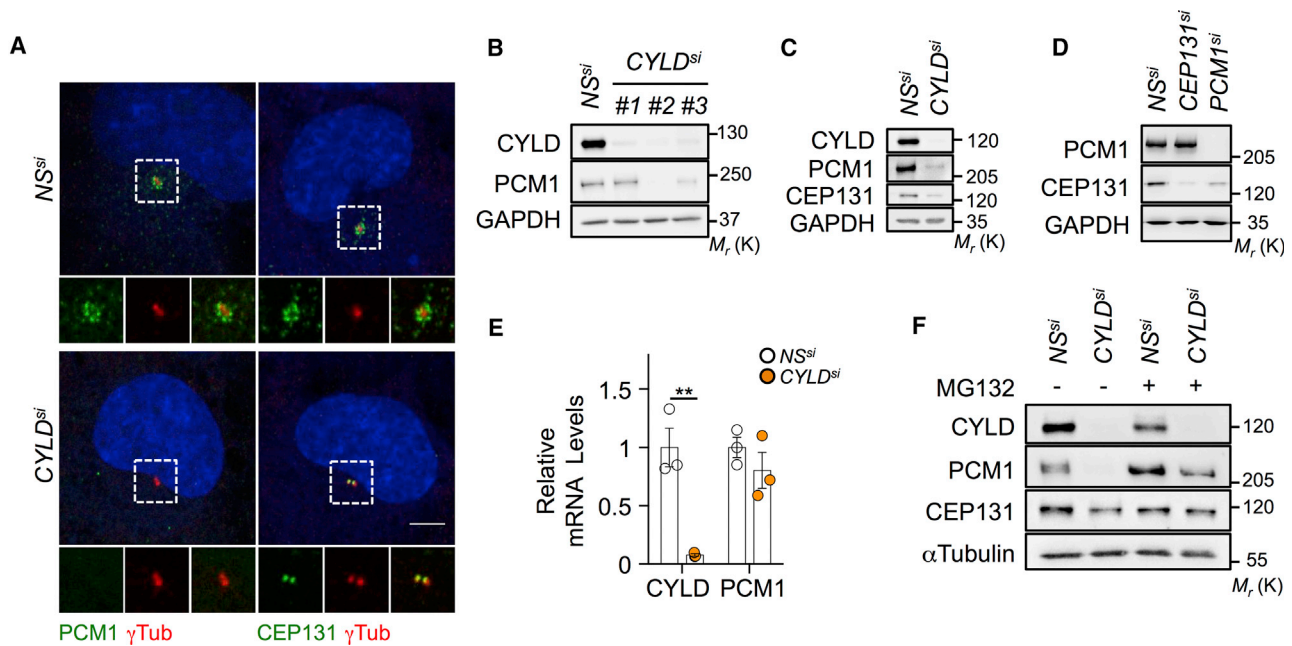


**Figure 3. CYLD Controls the Proteostasis of Centriolar Satellites**

(A) Confocal micrographs of RPE-1 cells transfected with siRNA for CYLD or scramble NS siRNA for 48 h, fixed and immunostained as indicated. Nuclei were illuminated with DAPI. Scale bar, 5  $\mu$ m. Data are representative of three independent experiments.

(B and C) RPE-1 cells were transfected with NS siRNA and with three individual CYLD-specific siRNA (B) or with CYLD siRNA#2 (C). Lys. were prepared and subjected to immunoblotting analysis with antibodies specific for the indicated proteins. Molecular weight markers are shown. Data are representative of three independent experiments.

(D) RPE-1 cells transfected with NS siRNA and with siRNA specific for CEP131 or PCM1 were analyzed as in (B). Data are representative of three independent experiments.

(E) RPE-1 cells were transfected as in (A). The transcription of CYLD and PCM1 was analyzed by qPCR (means  $\pm$  SEM, technical triplicates; \*\*p < 0.01; ns, nonsignificant [ANOVA]).

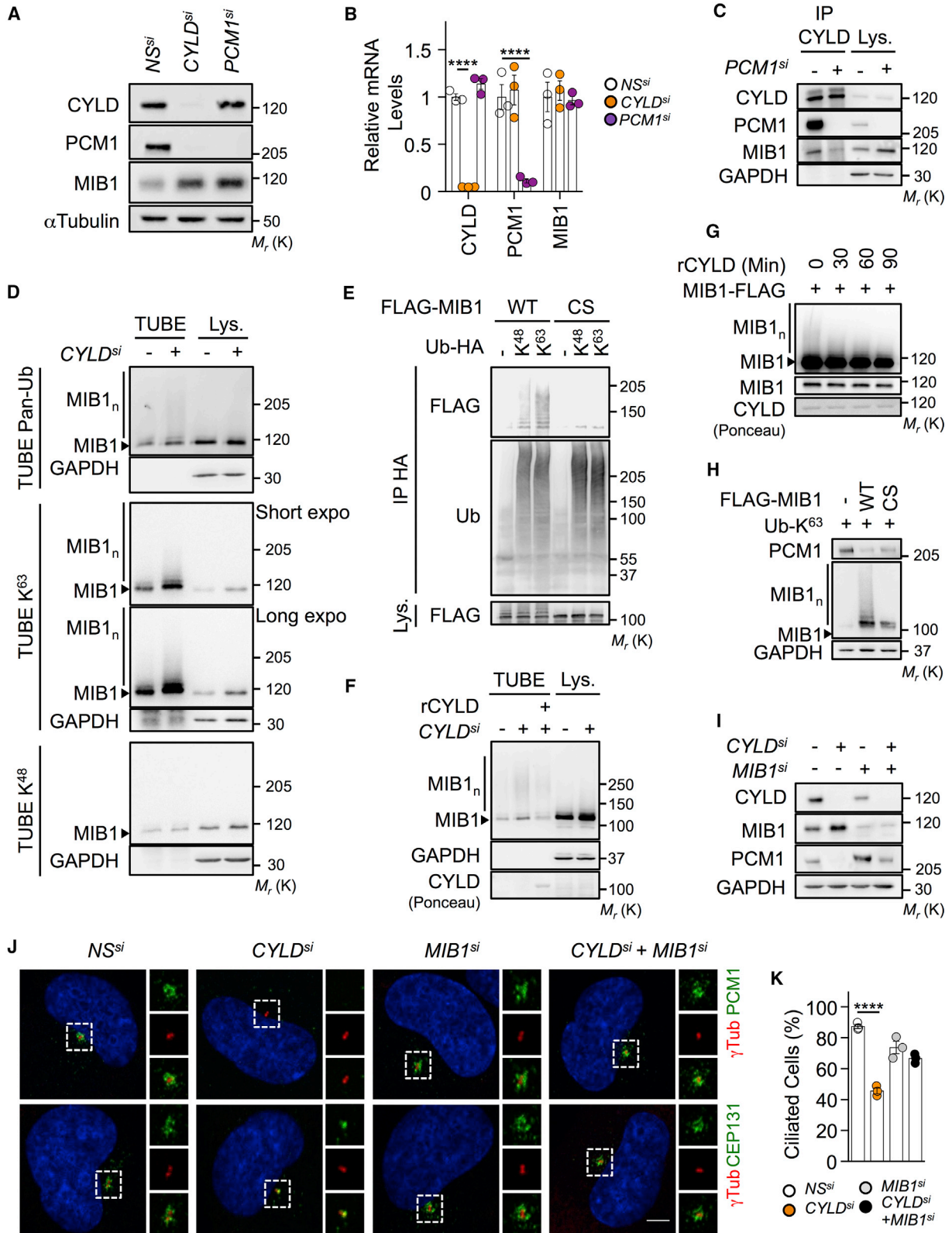
(F) RPE-1 cells as in (A) were treated with 25  $\mu$ M of MG132 for 6 h prior analysis by immunoblotting. The presented data are representative of three independent experiments.

with the specificity of CYLD for K<sup>63</sup>-linked ubiquitin chains (Komander et al., 2009). Of note, MIB1 K<sup>63</sup> ubiquitination was accompanied by a decrease in PCM1 abundance (Figure 4H). It should be stressed that our attempts to overexpress a catalytically dead CYLD remained unsuccessful. Lastly, we investigated the impact of SPATA2, as it was proposed to enhance CYLD activity (Elliott et al., 2016; Kupka et al., 2016; Schlicher et al., 2016; Wagner et al., 2016). However, SPATA2 silencing did not significantly alter the abundance of MIB1 and PCM1, suggesting SPATA2-independent functions for CYLD in this context (Figures S4F and S4G). Further supporting this idea, *Spata2* knockout mice do not display the characteristic ciliopathies-related symptoms seen in *Cyld* knockout animals (Wei et al., 2017). Altogether, our data suggest that CYLD removes K<sup>63</sup>-linked ubiquitin chains bound to MIB1.

To gain more functional insights, we next examined the interplay between CYLD and MIB1 on centriolar satellites homeostasis. We found that knocking down MIB1 in CYLD-silenced cells prevented PCM1 disappearance, restored the centriolar satellites subcellular organization, and re-enabled the cells to form primary cilia upon serum starvation (Figures 4I–4K and S4H). Collectively, our data suggest that CYLD deubiquitinates and prevents the E3 ligase MIB1 from promoting PCM1 proteasomal degradation.

Taken together, we provide evidence that a subset of CYLD interacts with centriolar satellites to maintain their proteostasis. CYLD is a pleiotropic DUB, which removes K<sup>63</sup>-linked ubiquitin chains from several substrates and regulates numerous cellular processes, including the activation of NF- $\kappa$ B or cell death by necroptosis (Harhaj and Dixit, 2012). CYLD has also been reported to localize in the cytosol, at the plasma membrane, or with the microtubule cytoskeleton and the midbody (Gao et al., 2008; Stegmeier et al., 2007; Urbé et al., 2012). Future works will therefore be required to define whether PCM1 and the centriolar satellites participate in some of the functions controlled by CYLD. This may expand the landscape of the cellular processes controlled by the centriolar satellites and PCM1 beyond ciliogenesis, together with regulation of neurogenesis (Ge et al., 2010), and GABARAP-dependent autophagy (Joachim et al., 2017).

Ubiquitination tightly regulates the function and the proteostasis of the centriolar satellites both in normal conditions and in response to stress (Tollenaere et al., 2015; Villumsen et al., 2013; Wang et al., 2016). A cornerstone of centriolar satellites regulation is MIB1. This E3 ligase was demonstrated to ubiquitinate the centriolar satellites linchpin PCM1, CEP131, as well as the centrosomal protein TALPID3, hence dismantling the



(legend on next page)

centriolar satellites and restricting ciliogenesis (Wang et al., 2016). Remarkably, PCM1 sequesters MIB1 to the centriolar satellites to curb its action (Tollenaere et al., 2015; Wang et al., 2016). Yet, how exactly PCM1 restrains MIB1 has remained unclear. We now show that the DUB CYLD is an integral centriolar satellites protein that removes K<sup>63</sup>-linked ubiquitin chains from MIB1 and finely tunes its abundance and activity. Depending on the cellular context, MIB1 can attach K<sup>11</sup>-, K<sup>29</sup>-, K<sup>48</sup>-, or K<sup>63</sup>-linked ubiquitin chains onto substrates and therefore drive different outcomes, such as protein degradation, stabilization, or signaling (Čajánek et al., 2015; Li et al., 2011). In the case of centriolar satellites, MIB1 K<sup>63</sup>-linked ubiquitination is linked to an increase in the degradation of some elements, including PCM1. This draws a striking parallel to the E3 ligases c-IAP1 and c-IAP2 in B-lymphocytes (Vallabhapurapu et al., 2008). The engagement of CD40 or BAFF-R mediates the K<sup>63</sup> ubiquitination and activation of c-IAPs, which subsequently mark TRAF3 with K<sup>48</sup>-linked ubiquitin chains and drive its proteasomal degradation (Vallabhapurapu et al., 2008).

Whether the decrease in protein amount observed in CYLD-silenced cell results from PCM1 loss and subsequent centriolar satellites dismantling or CYLD controls the proteostasis of additional centriolar satellites proteins will require additional studies. A number of centriolar satellites components also localize to the centrosome and the cilium complex (Tollenaere et al., 2015), and reports have found CYLD at the centrosome (Eguether et al., 2014; Yang et al., 2014). Although our data support a localization of CYLD at the centriolar satellites, they do not exclude centrosomal placement, and the data fit with the idea that centriolar satellites serve as cargo to transport centrosomal proteins (Dammernann and Merdes, 2002). It is likely that CYLD is not the sole DUB in charge of maintaining the integrity of the centriolar satellites. For instance, the X-linked DUB USP9X was recently identified as a CEP131-binding partner essential for maintaining the level of CEP131 and PCM1 (Han et al., 2019; Li et al., 2017; Wang et al., 2017). In keeping with this idea, mutations in USP9X cause a defect in cilia formation and lead to ciliopathies

in humans (Reijnders et al., 2016). Future work will be required to define whether CYLD and USP9X cooperate to orchestrate the proteostasis of the centriolar satellites.

In summary, our data provide insight into how reversible ubiquitination regulates the centriolar satellites homeostasis and may offer new opportunities to modulate ciliogenesis.

## STAR★METHODS

Detailed methods are provided in the online version of this paper and include the following:

- KEY RESOURCES TABLE
- CONTACT FOR REAGENT AND RESOURCE SHARING
- EXPERIMENTAL MODEL AND SUBJECT DETAILS
- METHOD DETAILS
  - Reagents
  - Plasmids, siRNA, and Transfections
  - Western Blotting, Immunoprecipitation, Tandem Ubiquitin Binding Entities, and Subcellular Fractionation
  - *In vitro* Deubiquitinating Enzyme Assay
  - Antibodies Used for Western Blotting and Immunoprecipitations
  - Mass Spectrometry
  - Immunofluorescence
  - qPCR
- QUANTIFICATION AND STATISTICAL ANALYSIS

## SUPPLEMENTAL INFORMATION

Supplemental Information can be found online at <https://doi.org/10.1016/j.celrep.2019.04.036>.

## ACKNOWLEDGMENTS

We thank H. Rogniaux (INRA BIBS platform, ONIRIS, Nantes, France) for expertise and technical support for proteomic analysis; B. Dynlacht, T. Toda, D. Komander, and P.R. Elliott for kindly providing reagents; A. Benmerah

### Figure 4. CYLD Prevents the E3 Ligase MIB1 from Dismantling Centriolar Satellites

(A) RPE-1 cells were transfected with siRNA for CYLD, PCM1, or scramble NS siRNA for 48 h. Cell Lys. were prepared and subjected to immunoblotting analysis with antibodies specific for the indicated proteins. Molecular weight markers are shown. Data are representative of three independent experiments.

(B) The transcription of CYLD, PCM1, and MIB1 was measured by qPCR analysis in cells as in (A). Histograms show means ± SEM of technical triplicates. \*\*\*\*p < 0.0001 (ANOVA).

(C) Cell Lys. from RPE-1 cells transfected with NS-siRNA or PCM1-siRNA for 48 h were subjected to IPs with antibodies against CYLD, and samples were then analyzed by immunoblotting as indicated. Data are representative of three independent experiments.

(D) Lys. from RPE-1 cells treated as in (A) were subjected to a TUBE pan-ubiquitin, TUBE-K<sup>63</sup>, or TUBE-K<sup>48</sup> pull-down, and immunoblotting was performed as indicated. MIB1 (arrowhead) and ubiquitinated MIB1 (MIB1<sub>n</sub>) are indicated. Data are representative of three independent experiments.

(E) HEK293T cells were transfected with plasmids encoding for FLAG-MIB1-wild type (WT) or FLAG-MIB1-CS together with HA-Ub-K<sup>48</sup> and HA-Ub-K<sup>63</sup>. Cell Lys. were prepared and subjected to IP prior analysis by immunoblotting as indicated. The dash (-) indicates an empty vector. Data are representative of two independent experiments.

(F) RPE-1 cells transfected with NS siRNA or CYLD-siRNA were lysed, and ubiquitinated proteins were purified by a TUBE pan-ubiquitin pull-down. Samples were treated or not with recombinant CYLD for 30 min and analyzed by immunoblotting as indicated. Data are representative of two independent experiments.

(G) FLAG-MIB1 ectopically expressed in HEK293T was purified by IP with FLAG antibodies and eluted using a FLAG peptide, prior incubation *in vitro* with recombinant CYLD for 0–90 min. Samples were then subjected to immunoblotting. Data are representative of three independent experiments.

(H) HEK293T were treated as in (E) and analyzed by immunoblotting as indicated.

(I) RPE-1 cells were transfected with siRNA for CYLD, MIB1, a combination of CYLD and MIB1, or NS siRNA for 48 h. Cell Lys. were prepared and subjected to immunoblotting as indicated. Data are representative of three independent experiments.

(J) Confocal microscopy analysis of RPE-1 cells as in (I). Nuclei were stained by DAPI. Scale bar, 5 μm. Data are representative of three independent experiments.

(K) RPE-1 cells as in (I) were serum starved for 24 h, fixed, and immunostained with antibodies specific to acetylated tubulin and to γTubulin. Ciliated cells were counted (means ± SEM of three independent experiments; n > 100 cells counted per samples; \*\*\*\*p < 0.0001 [ANOVA]).

for advice; M. Fernandez for technical assistance; and the Micropicell facility (SFR Santé François Bonamy, Nantes, France). This research was funded by an International Program for Scientific Cooperation (PICS, CNRS), Fondation ARC pour la recherche sur le Cancer (N.B.), Ligue nationale contre le cancer comités de Loire-Atlantique, Maine et Loire, Vendée (J.G., N.B.), Région Pays de la Loire et Nantes Métropole under Connect Talent Grant (J.G.), the National Research Agency under the Programme d'Investissements d'Avenir (ANR-16-IDEX-0007), and the SIRIC ILIAD (INCa-DGOS-Inserm\_12558). T.D. is a PhD fellow funded by Nantes Métropole and G.A.G. and A.T. hold postdoctoral fellowships from Fondation de France and Fondation ARC, respectively. Team projects are funded by Equipe Labellisée Fondation pour la Recherche Médicale (FRM DEQ20180339184).

## AUTHOR CONTRIBUTIONS

Conceptualization, T.D., G.A.-G., A.T., K.T., and N.B.; Methodology, T.D., G.A.-G., A.T., K.T., and N.B.; Investigation, T.D., G.A.-G., A.T., K.T., and N.B.; Supervision, J.G.; Writing – Original Draft, T.D. and N.B.; Writing – Review & Editing, T.D., G.A.-G., A.T., J.G., and N.B.; Funding Acquisition, J.G. and N.B.

## DECLARATION OF INTERESTS

The authors declare no competing interests.

Received: October 25, 2018

Revised: March 18, 2019

Accepted: April 5, 2019

Published: May 7, 2019

## REFERENCES

- André-Grégoire, G., Bidère, N., and Gavard, J. (2018). Temozolomide affects extracellular vesicles released by glioblastoma cells. *Biochimie* 155, 11–15.
- Čajánek, L., Glatter, T., and Nigg, E.A. (2015). The E3 ubiquitin ligase Mib1 regulates Plk4 and centriole biogenesis. *J. Cell Sci.* 128, 1674–1682.
- Dammermann, A., and Merdes, A. (2002). Assembly of centrosomal proteins and microtubule organization depends on PCM-1. *J. Cell Biol.* 159, 255–266.
- Dubois, S.M., Alexia, C., Wu, Y., Leclair, H.M., Leveau, C., Schol, E., Fest, T., Tarte, K., Chen, Z.J., Gavard, J., and Bidère, N. (2014). A catalytic-independent role for the LUBAC in NF- $\kappa$ B activation upon antigen receptor engagement and in lymphoma cells. *Blood* 123, 2199–2203.
- Eguether, T., Ermolaeva, M.A., Zhao, Y., Bonnet, M.C., Jain, A., Pasparakis, M., Courtois, G., and Tassin, A.-M. (2014). The deubiquitinating enzyme CYLD controls apical docking of basal bodies in ciliated epithelial cells. *Nat. Commun.* 5, 4585.
- Elliott, P.R., Leske, D., Hrdinka, M., Bagola, K., Fiil, B.K., McLaughlin, S.H., Wagstaff, J., Volkmar, N., Christianson, J.C., Kessler, B.M., et al. (2016). SPATA2 links CYLD to LUBAC, activates CYLD, and controls LUBAC signaling. *Mol. Cell* 63, 990–1005.
- Gao, J., Huo, L., Sun, X., Liu, M., Li, D., Dong, J.-T., and Zhou, J. (2008). The tumor suppressor CYLD regulates microtubule dynamics and plays a role in cell migration. *J. Biol. Chem.* 283, 8802–8809.
- Ge, X., Frank, C.L., Calderon de Anda, F., and Tsai, L.-H. (2010). Hook3 interacts with PCM1 to regulate pericentriolar material assembly and the timing of neurogenesis. *Neuron* 65, 191–203.
- Gomez-Ferrera, M.A., Bashkurov, M., Mullin, M., Gingras, A.-C., and Pelletier, L. (2012). CEP192 interacts physically and functionally with the K63-deubiquitinase CYLD to promote mitotic spindle assembly. *Cell Cycle* 11, 3555–3558.
- Han, K.-J., Wu, Z., Pearson, C.G., Peng, J., Song, K., and Liu, C.-W. (2019). Deubiquitylase USP9X maintains centriolar satellite integrity by stabilizing pericentriolar material 1 protein. *J. Cell Sci.* 132, jcs221663.
- Harhaj, E.W., and Dixit, V.M. (2012). Regulation of NF- $\kappa$ B by deubiquitinases. *Immunol. Rev.* 246, 107–124.
- Hjerpe, R., Aillet, F., Lopitz-Otsoa, F., Lang, V., England, P., and Rodriguez, M.S. (2009). Efficient protection and isolation of ubiquitylated proteins using tandem ubiquitin-binding entities. *EMBO Rep.* 10, 1250–1258.
- Hori, A., and Toda, T. (2017). Regulation of centriolar satellite integrity and its physiology. *Cell. Mol. Life Sci.* 74, 213–229.
- Hori, A., Barnouin, K., Sniijders, A.P., and Toda, T. (2016). A non-canonical function of Plk4 in centriolar satellite integrity and ciliogenesis through PCM1 phosphorylation. *EMBO Rep.* 17, 326–337.
- Hrdinka, M., and Gyrd-Hansen, M. (2017). The Met1-linked ubiquitin machinery: Emerging themes of (de)regulation. *Mol. Cell* 68, 265–280.
- Jin, W., Chang, M., Paul, E.M., Babu, G., Lee, A.J., Reiley, W., Wright, A., Zhang, M., You, J., and Sun, S.-C. (2008). Deubiquitinating enzyme CYLD negatively regulates RANK signaling and osteoclastogenesis in mice. *J. Clin. Invest.* 118, 1858–1866.
- Joachim, J., Razi, M., Judith, D., Wirth, M., Calamita, E., Encheva, V., Dynlacht, B.D., Sniijders, A.P., O'Reilly, N., Jefferies, H.B.J., and Tooze, S.A. (2017). Centriolar satellites control GABARAP ubiquitination and GABARAP-mediated autophagy. *Curr. Biol.* 27, 2123–2136, e1–e7.
- Kim, J., Krishnaswami, S.R., and Gleeson, J.G. (2008). CEP290 interacts with the centriolar satellite component PCM-1 and is required for Rab8 localization to the primary cilium. *Hum. Mol. Genet.* 17, 3796–3805.
- Komander, D., and Rape, M. (2012). The ubiquitin code. *Annu. Rev. Biochem.* 81, 203–229.
- Komander, D., Reyes-Turcu, F., Licchesi, J.D.F., Odenwaelder, P., Wilkinson, K.D., and Barford, D. (2009). Molecular discrimination of structurally equivalent Lys 63-linked and linear polyubiquitin chains. *EMBO Rep.* 10, 466–473.
- Kupka, S., De Miguel, D., Draber, P., Martino, L., Surinova, S., Rittinger, K., and Walczak, H. (2016). SPATA2-mediated binding of CYLD to HOIP enables CYLD recruitment to signaling complexes. *Cell Rep.* 16, 2271–2280.
- Lecland, N., and Merdes, A. (2018). Centriolar satellites prevent uncontrolled degradation of centrosome proteins: a speculative review. *Cell Stress* 2, 20–24.
- Li, S., Wang, L., Berman, M., Kong, Y.-Y., and Dorf, M.E. (2011). Mapping a dynamic innate immunity protein interaction network regulating type I interferon production. *Immunity* 35, 426–440.
- Li, X., Song, N., Liu, L., Liu, X., Ding, X., Song, X., Yang, S., Shan, L., Zhou, X., Su, D., et al. (2017). USP9X regulates centrosome duplication and promotes breast carcinogenesis. *Nat. Commun.* 8, 14866.
- Lim, K.L., Chew, K.C.M., Tan, J.M.M., Wang, C., Chung, K.K.K., Zhang, Y., Tanaka, Y., Smith, W., Engelender, S., Ross, C.A., et al. (2005). Parkin mediates nonclassical, proteasomal-independent ubiquitination of synphilin-1: implications for Lewy body formation. *J. Neurosci.* 25, 2002–2009.
- Malicki, J.J., and Johnson, C.A. (2017). The cilium: cellular antenna and central processing unit. *Trends Cell Biol.* 27, 126–140.
- Mellacheruvu, D., Wright, Z., Couzens, A.L., Lambert, J.-P., St-Denis, N.A., Li, T., Miteva, Y.V., Hauri, S., Sardi, M.E., Low, T.Y., et al. (2013). The CRAPome: a contaminant repository for affinity purification-mass spectrometry data. *Nat. Methods* 10, 730–736.
- Mevissen, T.E.T., and Komander, D. (2017). Mechanisms of deubiquitinase specificity and regulation. *Annu. Rev. Biochem.* 86, 159–192.
- Reijnders, M.R.F., Zachariadis, V., Latour, B., Jolly, L., Mancini, G.M., Pfundt, R., Wu, K.M., van Ravenswaaij-Arts, C.M.A., Veenstra-Knol, H.E., Anderlid, B.-M.M., et al.; DDD Study (2016). De Novo loss-of-function mutations in USP9X cause a female-specific recognizable syndrome with developmental delay and congenital malformations. *Am. J. Hum. Genet.* 98, 373–381.
- Schlicher, L., Wissler, M., Preiss, F., Brauns-Schubert, P., Jakob, C., Dumit, V., Borner, C., Dengjel, J., and Maurer, U. (2016). SPATA2 promotes CYLD activity and regulates TNF-induced NF- $\kappa$ B signaling and cell death. *EMBO Rep.* 17, 1485–1497.
- Stegemeier, F., Sowa, M.E., Nalepa, G., Gygi, S.P., Harper, J.W., and Elledge, S.J. (2007). The tumor suppressor CYLD regulates entry into mitosis. *Proc. Natl. Acad. Sci. USA* 104, 8869–8874.

- Tollenaere, M.A.X., Villumsen, B.H., Blasius, M., Nielsen, J.C., Wagner, S.A., Bartek, J., Beli, P., Mailand, N., and Bekker-Jensen, S. (2015). p38- and MK2-dependent signalling promotes stress-induced centriolar satellite remodelling via 14-3-3-dependent sequestration of CEP131/AZI1. *Nat. Commun.* **6**, 10075.
- Trompouki, E., Tsagaratou, A., Kosmidis, S.K., Dollé, P., Qian, J., Kontoyianis, D.L., Cardoso, W.V., and Mosialos, G. (2009). Truncation of the catalytic domain of the cylindromatosis tumor suppressor impairs lung maturation. *Neoplasia* **11**, 469–476.
- Urbé, S., Liu, H., Hayes, S.D., Heride, C., Rigden, D.J., and Clague, M.J. (2012). Systematic survey of deubiquitinase localization identifies USP21 as a regulator of centrosome- and microtubule-associated functions. *Mol. Biol. Cell* **23**, 1095–1103.
- Vallabhapurapu, S., Matsuzawa, A., Zhang, W., Tseng, P.-H., Keats, J.J., Wang, H., Vignali, D.A.A., Bergsagel, P.L., and Karin, M. (2008). Nonredundant and complementary functions of TRAF2 and TRAF3 in a ubiquitination cascade that activates NIK-dependent alternative NF- $\kappa$ B signaling. *Nat. Immunol.* **9**, 1364–1370.
- Villumsen, B.H., Danielsen, J.R., Povlsen, L., Sylvestersen, K.B., Merdes, A., Beli, P., Yang, Y.-G., Choudhary, C., Nielsen, M.L., Mailand, N., and Bekker-Jensen, S. (2013). A new cellular stress response that triggers centriolar satellite reorganization and ciliogenesis. *EMBO J.* **32**, 3029–3040.
- Wagner, S.A., Satpathy, S., Beli, P., and Choudhary, C. (2016). SPATA2 links CYLD to the TNF- $\alpha$  receptor signaling complex and modulates the receptor signaling outcomes. *EMBO J.* **35**, 1868–1884.
- Wang, L., Lee, K., Malonis, R., Sanchez, I., and Dynlacht, B.D. (2016). Tethering of an E3 ligase by PCM1 regulates the abundance of centrosomal KIAA0586/Talpid3 and promotes ciliogenesis. *eLife* **5**, e12950.
- Wang, Q., Tang, Y., Xu, Y., Xu, S., Jiang, Y., Dong, Q., Zhou, Y., and Ge, W. (2017). The X-linked deubiquitinase USP9X is an integral component of centrosome. *J. Biol. Chem.* **292**, 12874–12884.
- Wei, R., Xu, L.W., Liu, J., Li, Y., Zhang, P., Shan, B., Lu, X., Qian, L., Wu, Z., Dong, K., et al. (2017). SPATA2 regulates the activation of RIPK1 by modulating linear ubiquitination. *Genes Dev.* **31**, 1162–1176.
- Wright, A., Reiley, W.W., Chang, M., Jin, W., Lee, A.J., Zhang, M., and Sun, S.-C. (2007). Regulation of early wave of germ cell apoptosis and spermatogenesis by deubiquitinating enzyme CYLD. *Dev. Cell* **13**, 705–716.
- Yang, Y., and Zhou, J. (2016). CYLD - a deubiquitylase that acts to fine-tune microtubule properties and functions. *J. Cell Sci.* **129**, 2289–2295.
- Yang, Y., Ran, J., Liu, M., Li, D., Li, Y., Shi, X., Meng, D., Pan, J., Ou, G., Aneja, R., et al. (2014). CYLD mediates ciliogenesis in multiple organs by deubiquitinating Cep70 and inactivating HDAC6. *Cell Res.* **24**, 1342–1353.

## STAR★METHODS

### KEY RESOURCES TABLE

REAGENT or RESOURCE	SOURCE	IDENTIFIER
<b>Antibodies</b>		
Acetylated Tubulin 6-11 B-1	Santa Cruz	Cat#sc-23950; RRID: AB_628409
CYLD (H-6)	Santa Cruz	Cat#sc-137139; RRID: AB_2261344
GAPDH (6C5)	Santa Cruz	Cat#sc-32233; RRID: AB_627679
HOIL1 (H-1)	Santa Cruz	Cat#sc-393754
Lck (3A5)	Santa Cruz	Cat#sc-433; RRID: AB_2784531
SPATA2 (B-7)	Santa Cruz	Cat#sc-515283
$\alpha$ Tubulin (TU-02)	Santa Cruz	Cat#sc-8035; RRID: AB_628408
$\gamma$ Tubulin (TU-30)	Santa Cruz	Cat#sc-51715; RRID: AB_630410
Ubiquitin (P4D1)	Santa Cruz	Cat#sc-8017; RRID: AB_2762364
CEP131	Bethyl Laboratories	Cat#A301-415A; RRID: AB_960949
HOIP	Bethyl Laboratories	Cat#A303-560A; RRID: AB_10949139
SHARPIN	Bethyl Laboratories	Cat#A303-559A; RRID: AB_10971166
SPATA2	Bethyl Laboratories	Cat#A302-493A; RRID: AB_1966056
SPATA2	Bethyl Laboratories	Cat#A302-494A; RRID: AB_1966055
USP34	Bethyl Laboratories	Cat#A300-824A; RRID: AB_2213353
HA.11	Biologend	Cat#901501; RRID: AB_2565006
CAP350	Abcam	Cat#ab219831
FLAG M2	Sigma	Cat#F1804; RRID: AB_262044
MIB1	Sigma	Cat#M5948; RRID: AB_1841007
$\gamma$ Tubulin (GTU-88)	Sigma	Cat#T6557; RRID: AB_477584
CYLD	Atlas	Cat#HPA050095; RRID: AB_2681013
<b>Chemicals, Peptides, and Recombinant Proteins</b>		
Opti-MEM	Life Technologies	Cat#11058021
F-12 Medium	Life Technologies	Cat#21331-020
DMEM	Life Technologies	Cat#21969-035
Prolong Gold anti-fade Mounting Media	Life Technologies	Cat#P36935
Lipofectamine RNAimax Transfection Reagent	Life Technologies	Cat#13778150
Nocodazole	Sigma	Cat#3140-18-9
PR-619	Selleckchem	Cat#A13190
Bortezomib	Selleckchem	Cat#S1013
MG-132	Cell Signaling Technology	Cat#A11043
recombinant CYLD	D. Komander	N/A
3X FLAG peptide	Sigma	Cat#F4799
<b>Critical Commercial Assays</b>		
Nuclei Pure Sucrose Cushion	Sigma	Cat#NUC201
FLAG-2 M2 Affinity Resin	Sigma	Cat#A2220
Agarose-Pan Ub TUBE	Life Sensors	Cat#UM401/UM402
FLAG-K <sup>48</sup> TUBE	Life Sensors	Cat#UM604
FLAG-K <sup>63</sup> TUBE	Life Sensors	Cat#UM-604
RNeasy Mini Kit	QIAGEN	Cat#74104
PerfeCTa SYBR Green SuperMix Low ROX	QuantaBio	Cat#95053
Micro BCA Protein Assay kit	Thermo Scientific	Cat#23235
Immobilon Western Chemiluminescent HRP substrate	Millipore	Cat#WBKLS0500

(Continued on next page)

<b>Continued</b>		
REAGENT or RESOURCE	SOURCE	IDENTIFIER
Experimental Models: Cell Lines		
hTERT RPE-1	ATCC	Cat#CRL-4000
U2OS	ATCC	Cat#40345
HEK293T	ATCC	Cat#CRL-3216
Jurkat E6.1	ATCC	Cat#PTS-TIB-152
HeLa	ATCC	Cat#CCL2
Oligonucleotides		
See <a href="#">Table S1</a> for siRNA sequences		N/A
Primer ACTBf: GGACTTCGAGCAAGAGATGG	Eurogentech	N/A
Primer ACTBr: AGCACTGTGTTGGCGTACAG	Eurogentech	N/A
Primer CYLdf: TGTGACAGCATGGACACCAC	Eurogentech	N/A
Primer CYLDr: CCCCCTCAGTCAAACCTTGA	Eurogentech	N/A
Primer HPRT1f: TGACACTGGCAAACAATGCA	Eurogentech	N/A
Primer HPRT1r: GGTCTTTTCACCAGCAAGCT	Eurogentech	N/A
Primer MIB1f: ATAACCGGGTGATGGTGAAG	Eurogentech	N/A
Primer MIB1r: ACAGAACCCTCTCACTCCCG	Eurogentech	N/A
Primer PCM1f: TTGAAGTGTGGAGCGGAAA	Eurogentech	N/A
Primer PCM1r: GTTGGGCACCCCAATCCATA	Eurogentech	N/A
Recombinant DNA		
pEGFP-hPCM1	T. Toda ( <a href="#">Hori et al., 2016</a> )	N/A
pFLAG-MIB1	B. Dynlacht ( <a href="#">Wang et al., 2016</a> )	N/A
pRK5-HA-Ubiquitin-WT	Addgene	Cat#17608
pRK5-HA-Ubiquitin-K48 only	Addgene	Cat#17605
pRK5-HA-Ubiquitin-K63 only	Addgene	Cat#17606
Software and Algorithms		
MASCOT server		N/A
STRING database	STRING	<a href="https://string-db.org/">https://string-db.org/</a>
Other		
NEON Transfection System	Thermo Fisher Scientific	Cat#MPK5000
Confocal Microscope	Nikon	Cat#A1R
LC-ESI-ORbitrap Velos Mass Spectrometer	Thermo Fisher Scientific	N/A
Thermocycler Stratagene MX3005P	Agilent	Cat#MX3005P

## CONTACT FOR REAGENT AND RESOURCE SHARING

Further information and requests for resources and reagents should be directed to and will be fulfilled by the Lead Contact, Nicolas Bidère ([nicolas.bidere@inserm.fr](mailto:nicolas.bidere@inserm.fr)).

## EXPERIMENTAL MODEL AND SUBJECT DETAILS

Human hTERT RPE-1, U2OS, HEK293T, HeLa, and Jurkat E6.1 cells were purchased from the American Type Culture Collection. hTERT RPE-1 (female) were cultured in Dulbecco's modified Eagle's F12 (DMEM:F12, Life Technologies) supplemented with 10% Fetal Bovine Serum (FBS) and Penicillin/Streptomycin (Life Technologies). HeLa (female) and HEK293T (fetus) cells were maintained in Dulbecco's modified Eagle's (DMEM, Life Technologies) supplemented with 10% FBS and Penicillin/Streptomycin. U2OS (female) were cultured in McCoy's 5a Medium Modified (Life Technologies) supplemented with 10% FBS and Penicillin/Streptomycin. Jurkat E6.1 (male) cells were grown with RPMI1640 (Life Technologies) supplemented with 10% FBS, HEPES (Life Technologies), Sodium Pyruvate (Life Technologies) and Penicillin/Streptomycin. All cell lines were maintained at 37°C with 5% CO<sub>2</sub>. Ciliogenesis was induced by washing and incubating RPE-1 cells in OPTI-MEM (Life Technologies) for 24 hours.

## METHOD DETAILS

### Reagents

Nocodazole (Sigma), PR619 (Selleckchem), MG132 (Cell Signaling Technology), and Bortezomib (Selleckchem) were used.

### Plasmids, siRNA, and Transfections

RPE-1, U2OS and HeLa cells were transfected with 10 pmol of individual siRNA, at a final concentration of 16.5 nM, using the Lipofectamine RNAiMAX Transfection Reagent (Invitrogen), according to the manufacturer's instructions. The following sequences (Invitrogen, Stealth) were used: CYLD #1, GAUUCUGCCUGGCUCUUCUUGACA (HSS102532); CYLD #2, GAAGUAGGAGAGUACUUGAAG AUGU (HSS102533); CYLD #3, ACGAAGACUGCUUUGUGAUGCAUUAU (HSS102534); PCM1, GCCUAACCCUUGCCGUUACG UUUUA (HSS107661); MIB1 #1, GGGUGAUCUUGUACAAGUUUGUUUAU (HSS126394); MIB1 #2, GGACAUUUGCUACCUGUU CUUUUAU (HSS126395); MIB1 #3, UCUCAAGUGGGAUUAUCCAGUAUUU (HSS126396); SPATA2 #1, CCUGCCUCAGCGCUUACCA UUAUGA (HSS114826); SPATA2 #2, UCGAGUGUGAGCAGAUGCAGAAA (HSS114828); SPATA2 #3, CCACCCAGCUCUCCCAU CUCGUGUA (HSS190646). The siRNA sequence targeting CEP131 was GUUGAGAUGCCCACGGCUATT, as previously described (Tollenaere et al., 2015). CYLD siRNA #2 and MIB1 siRNA #2 were used unless otherwise specified. HEK293T cells were transfected using a standard calcium phosphate protocol. RPE-1 cells were transfected with 0.5  $\mu$ g of pEGFP-hPCM1 kindly provided by T. Toda (Hori et al., 2016) using the Neon Transfection System (Thermo Fisher) according to the manufacturer's instructions using the following electroporation parameters: 1400 V, 20 ms, 1 pulse. pRK5-HA-Ubiquitin plasmids (WT, K<sup>48</sup>-only, K<sup>63</sup>-only) were a gift from Ted Dawson (Addgene plasmids#17605, 17606, 17608) (Lim et al., 2005).

### Western Blotting, Immunoprecipitation, Tandem Ubiquitin Binding Entities, and Subcellular Fractionation

Cells were washed with ice-cold PBS prior cell lysis with TNT buffer [50 mM Tris-HCl (pH 7.4), 150 mM NaCl, 1% Triton X-100, 1% Igepal, 2 mM EDTA] or RIPA buffer [25 mM Tris-HCl (pH 7.4), 150 mM NaCl, 0.1% SDS, 0.5% Na-Deoxycholate, 1% NP-40, 1 mM EDTA] supplemented with protease inhibitors (Pierce) for 30 minutes on ice. Samples were cleared by centrifugation at 10,000g and protein concentration determined by BCA (Thermo Fisher Scientific). 5-10  $\mu$ g proteins were resolved by SDS-PAGE and transferred to nitrocellulose membranes (GE Healthcare). Immunoprecipitations were performed as previously described (Dubois et al., 2014). Briefly, samples lysed with TNT buffer were precleared with Protein G Sepharose (Sigma) for 30 minutes, prior incubation with 1  $\mu$ g antibodies and Protein G Sepharose for 1-2 hours at 4°C. Antibodies to Lck and USP34 served as isotype-matched controls for CYLD and CEP131, respectively.

The pull-down of Pan-, K<sup>48</sup>- and K<sup>63</sup>-linked ubiquitinated proteins was performed with agarose and FLAG-tagged TUBE (Life Sensors), following the manufacturer's instructions. Briefly, for Pan-ubiquitin, cells were collected, washed twice with PBS and lysed with TNT buffer supplemented with protease inhibitors (Pierce) and 100  $\mu$ M of PR619. Clarified lysates were incubated for 30 minutes on uncoupled agarose to remove non-specific binding and 2 hours on equilibrated Agarose-TUBE under rotation. Resin was washed 3 times with TBS-T [200 mM Tris-HCl pH 8.0, 0.15 M NaCl, 0.1% Tween-20] and resolved by SDS-PAGE. For K<sup>48</sup>- and K<sup>63</sup>-TUBE, cells were collected, washed twice in PBS and lysed with lysis buffer [100 mM Tris-HCl pH 8.0, 0.15 M NaCl, 5 mM EDTA, 1% Igepal, 0.5% Triton X-100] supplemented with protease inhibitors (Pierce), 100  $\mu$ M of PR619 and 250 nM of FLAG-TUBE K<sup>63</sup> or 250 nM of FLAG-TUBE K<sup>48</sup>. Clarified lysates were diluted with reaction buffer to reduce concentration of Igepal to 0.1% and Triton X-100 to 0.05%. Reaction was incubated on ice for 1 hour and lysates were added to equilibrated FLAG M2 Affinity Resin (Sigma) for 2 hours under rotation. Resin was washed 3 times with wash buffer [100 mM Tris-HCl pH 8.0, 0.15 M NaCl, 5 mM EDTA, 0.05% Igepal] and resolved by SDS-PAGE.

For cell fractionation, 10-20  $\times$  10<sup>6</sup> cells were incubated with 180  $\mu$ L of Buffer A [10 mM HEPES (pH 7.9), 10 mM KCl, 0.1 mM EDTA, 0.1 mM EGTA, 1 mM DTT, 1 mM Na<sub>3</sub>VO<sub>4</sub>, protease inhibitors] on ice for 5 minutes. 12.5  $\mu$ L of Buffer A containing 10% Igepal was added for another 5 minutes and followed by a centrifugation at 2,500g for 3 minutes. Supernatants were further spun at 25,000g for 30 minutes to obtain a cytosolic fraction (S25). Pellets containing nuclei, centriolar satellites and centrosomes were further centrifuged on a sucrose gradient (Nuclei Pure Sucrose Cushion, Sigma) at 20,000g for 45 minutes. The resulting pellets were lysed with 30  $\mu$ L of Buffer C [20 mM HEPES (pH 7.9), 400 mM NaCl, 1 mM EDTA, 1 mM EGTA, 1 mM DTT, 1 mM Na<sub>3</sub>VO<sub>4</sub>, protease inhibitors], and cleared by a 10,000g centrifugation. For the discontinuous sucrose gradient, 40  $\times$  10<sup>6</sup> cells were washed with ice-cold PBS, lysed with lysis buffer [50 mM Tris pH 8.0, 150 mM NaCl, 1 mM EDTA, 1 mM MgCl<sub>2</sub>, 10% glycerol, 0.5% NP-40 Igepal, 1 mM DTT, protease inhibitors] for 30 minutes and clarified by centrifugation at 1,500g for 5 minutes at 4°C according to (Kim et al., 2008). In brief, supernatants were layered on a discontinuous sucrose gradient (10, 20, 30, 40 and 50%) and ultra-centrifugated at 100,000g at 4°C for 150 minutes. Ten fractions were collected from the bottom, washed in salt solution, centrifugated at 30,000g at 4°C for 10 minutes and resolved by SDS-PAGE.

### In vitro Deubiquitinating Enzyme Assay

To produce ectopic MIB1, HEK293T cells were transfected with a plasmid encoding for MIB1-FLAG kindly provided by B. Dynlacht (Wang et al., 2016). After 24 hours, cell lysates were incubated with FLAG-M2 Affinity Resin (Sigma) under rotation for 2 hours at 4°C. MIB1 was eluted using 3X-FLAG Peptide (Sigma) at 100  $\mu$ g.mL<sup>-1</sup>. In vitro DUB assay was performed as in (Komander et al., 2009). Recombinant CYLD, kindly provided by D. Komander, was diluted at 0.2  $\mu$ g.mL<sup>-1</sup> in [150 mM NaCl, 25 mM Tris-HCl (pH 7.4) and

10 mM DTT] and incubated at room temperature for 10 minutes. In a 30  $\mu$ L reaction, 15  $\mu$ L of diluted CYLD was added to MIB1 and 3  $\mu$ L of 10 X DUB buffer [500 mM NaCl, 500 mM Tris-HCl (pH 7.4) and 50 mM DTT] and incubated at 37°C. At given time point, 8  $\mu$ L of reaction sample were mixed with 8  $\mu$ L Laemmli 2X buffer (Invitrogen) and resolved by SDS-PAGE.

### Antibodies Used for Western Blotting and Immunoprecipitations

Antibodies specific for the following proteins were purchased from Santa Cruz Biotechnology: CYLD (H-6), GAPDH (6C5), HOIL1 (H-1), Lck (3A5), SPATA2 (B-7),  $\alpha$ Tubulin (TU-02),  $\gamma$ Tubulin (TU-30), and Ubiquitin (P4D1). Antibodies specific for CEP131 (A301-415A), HOIP (A303-560A), USP34 (A300-824A), SHARPIN (A303-599A), and SPATA2 (A302-494A) were from Bethyl Laboratories. Antibodies against MIB1 (M5948), and FLAG (F1804) were from Sigma. Anti-HA (HA.11) antibodies were from BioLegend.

### Mass Spectrometry

Mass spectrometry analysis was performed with the BIBS facility (INRA Research Unit BIA, Nantes, France). RPE-1 lysates were subjected to immunoprecipitation using an antibody against CYLD. Briefly, 60. 10<sup>6</sup> non-starved RPE-1 cells were collected, washed in PBS, lysed in TNT buffer supplemented with protease inhibitors (Pierce) on ice for 30 minutes and lysates were cleared by centrifugation at 10,000g for 10 minutes. Lysates were incubated with Protein G Sepharose (Sigma) alone under rotation for 30 minutes as a “pre-clear” stage and further incubated with Protein G Sepharose and 5  $\mu$ g of CYLD antibody under rotation for 2 hours. Beads were collected and washed 4 times with TNT buffer. Proteins were resolved by SDS-PAGE and a Coomassie Blue staining was performed. Bands were hydrolysed with trypsin and the released peptides analyzed by LC-MS/MS using LC-ESI-ORbitrap Velos mass spectrometer (ThermoFisher). Spectra obtained were processed using MASCOT server and compared to UniprotHuman bank for protein identification. All proteins were ranked according to MASCOT score and proteins with at least two peptides above MASCOT threshold or a single peptide of individual score > 50 with a p value better than 10<sup>-5</sup> were conserved. Queries matched correspond to the number of MS/MS spectra identified for a protein. Single peptide score (also termed ions score) were calculated following  $-10\log(P)$  where P is the probability that an observed match is a random event. Here, the significance threshold (P) chosen was 0.05. The protein score is calculated as the sum of all unique peptide scores for said protein. Mass spectrometry identified proteins were analyzed for Cellular Component (GO) using STRING database (free online software <https://string-db.org/> version 10.5) with medium confidence score (0.400) setting (André-Grégoire et al., 2018). Contaminants, transcription machinery, nuclear and ribosomal proteins were excluded (Mellacheruvu et al., 2013).

### Immunofluorescence

Cells were fixed in 4% paraformaldehyde for 12 minutes at room temperature, incubated with ice-cold methanol for 2 minutes and quenched 10 minutes with PBS/100 mM glycine. Fixed cells were incubated 60 minutes with primary antibodies and 60 minutes with secondary antibodies in PBS 1X-0.2% BSA-0.05% Saponin. The following primary antibodies were used: CYLD (Atlas antibodies, HPA050095), MIB1 (Sigma, M5948),  $\gamma$ Tubulin (Sigma, GTU88), acetylated Tubulin (Santa Cruz Biotechnology, 6-11 B-1), CEP131 (Bethyl, A301-415A), SPATA2 (Bethyl, A302-493A), and CAP350 (Abcam, ab219831). Coverslips were sealed with Prolong gold anti-fade mounting media (Life Technologies) and nuclei were counterstained with 4',6-diamidino-2-phenylindole (DAPI). Confocal images were acquired with a Nikon A1R confocal microscope using the NIS-Element software. Structure illumination microscopy (SIM) images were acquired on a Nikon N-SIM microscope (MicroPicell, SFR François Bonamy, France). Images were reconstructed in 3D using the NIS-Element Software from Z stacks of 0.12  $\mu$ m taken using a 100x oil-immersion lens with a 1.49 numerical aperture. Images were processed using Fiji software. To disrupt the microtubule, RPE-1 cells were incubated with 2  $\mu$ g.mL<sup>-1</sup> nocodazole for two hours prior to fixation.

### qPCR

RNA was extracted using the RNeasy Mini Kit (QIAGEN) following manufacturer's instructions. Equal amounts of RNA were reverse transcribed using the Maxima Reverse Transcriptase kit (ThermoFisher) and 30 ng of the resulting cDNA was amplified by qPCR using PerfeCTa SYBR Green SuperMix Low ROX (QuantaBio). Data was analyzed using the 2<sup>- $\Delta\Delta$ Ct</sup> method and normalized by the house-keeping genes ACTB, HPRT1. The following primers were used: PCM1 forward: TTGAAGTGTGGAGCGGGAAA, PCM1 reverse: GTTGGGCACCCCAATCCATA, CYLD forward: TGTGACAGCATGGACACCAC, CYLD reverse: CCCCCTCAGTGAAACCTTGA, MIB1 forward: ATAACCGGGTGATGGTGGAAG, MIB1 reverse: ACAGAACCTCTCACTTCCCG, ACTB forward: GGACTTCGAGCAAGAG ATGG, ACTB reverse: AGCACTGTGTTGGCGTACAG, HPRT1 forward: TGACACTGGCAAAACAATGCA, HPRT1 reverse: GGTCC TTTTCACCAGCAAGCT.

### QUANTIFICATION AND STATISTICAL ANALYSIS

The number of independent biological repeats is shown in the figure legends. No samples were excluded in the analysis. Results are shown as mean  $\pm$  SEM. Statistical analyses were performed using GraphPad Prism 7 (GraphPad software) using one-way analysis of variance (ANOVA).

**Cell Reports, Volume 27**

**Supplemental Information**

**CYLD Regulates Centriolar Satellites Proteostasis  
by Counteracting the E3 Ligase MIB1**

**Tiphaine Douanne, Gwennan André-Grégoire, An Thys, Kilian Trillet, Julie Gavard, and Nicolas Bidère**

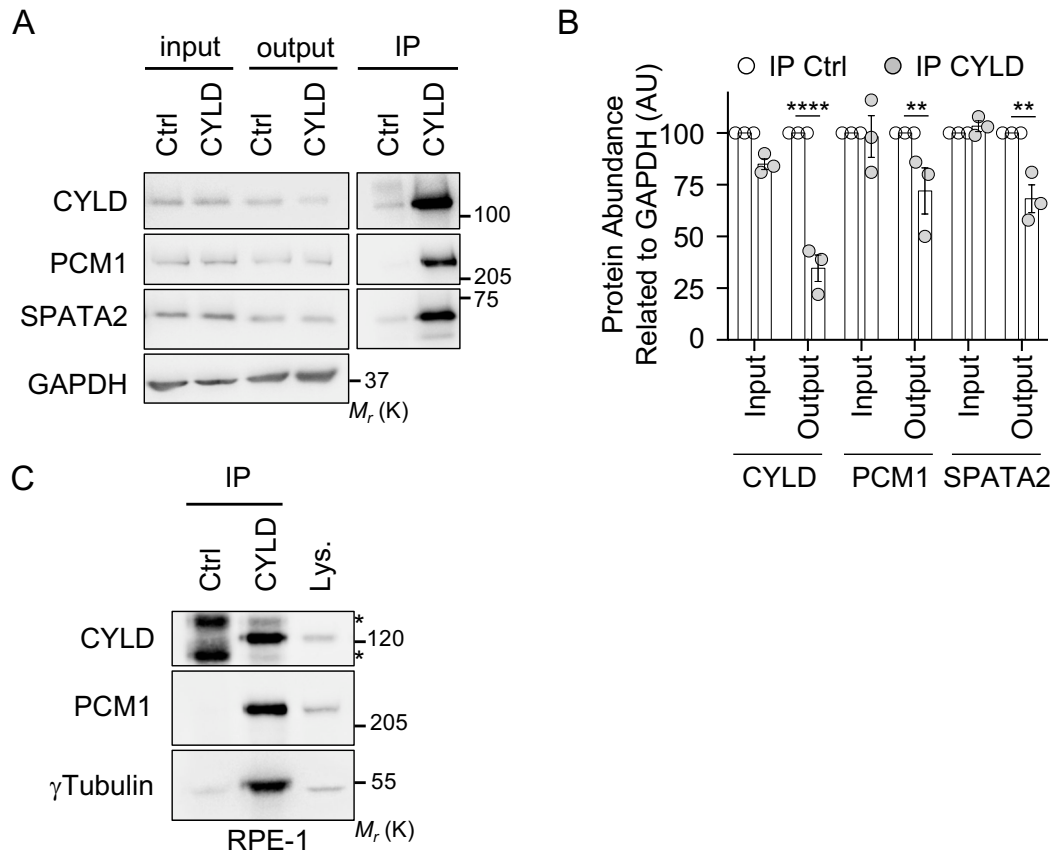


**Figure S1. CYLD binds Centriolar Satellites Components, Related to Figure 1.**

**A**, RPE-1 cells were lysed and immunoprecipitations (IP) were performed with antibodies to CYLD or with control unrelated (Ctrl) antibodies, and samples were analyzed by immunoblotting as indicated. Identical volumes of input and output lysates were also collected. Molecular weight markers are shown. **B**, The intensities of bands shown in panel (A) were quantified, and the ratios of the intensities of the indicated bands normalized to GAPDH were calculated. Shown are mean  $\pm$  SEM of three independent experiments. \*\*\*\* $P < 0.0001$ ; \*\* $P < 0.01$  (ANOVA). AU, arbitrary units. **C**, Cell lysates (Lys.) from RPE-1 cells were analyzed as in (A). \* indicates nonspecific bands.

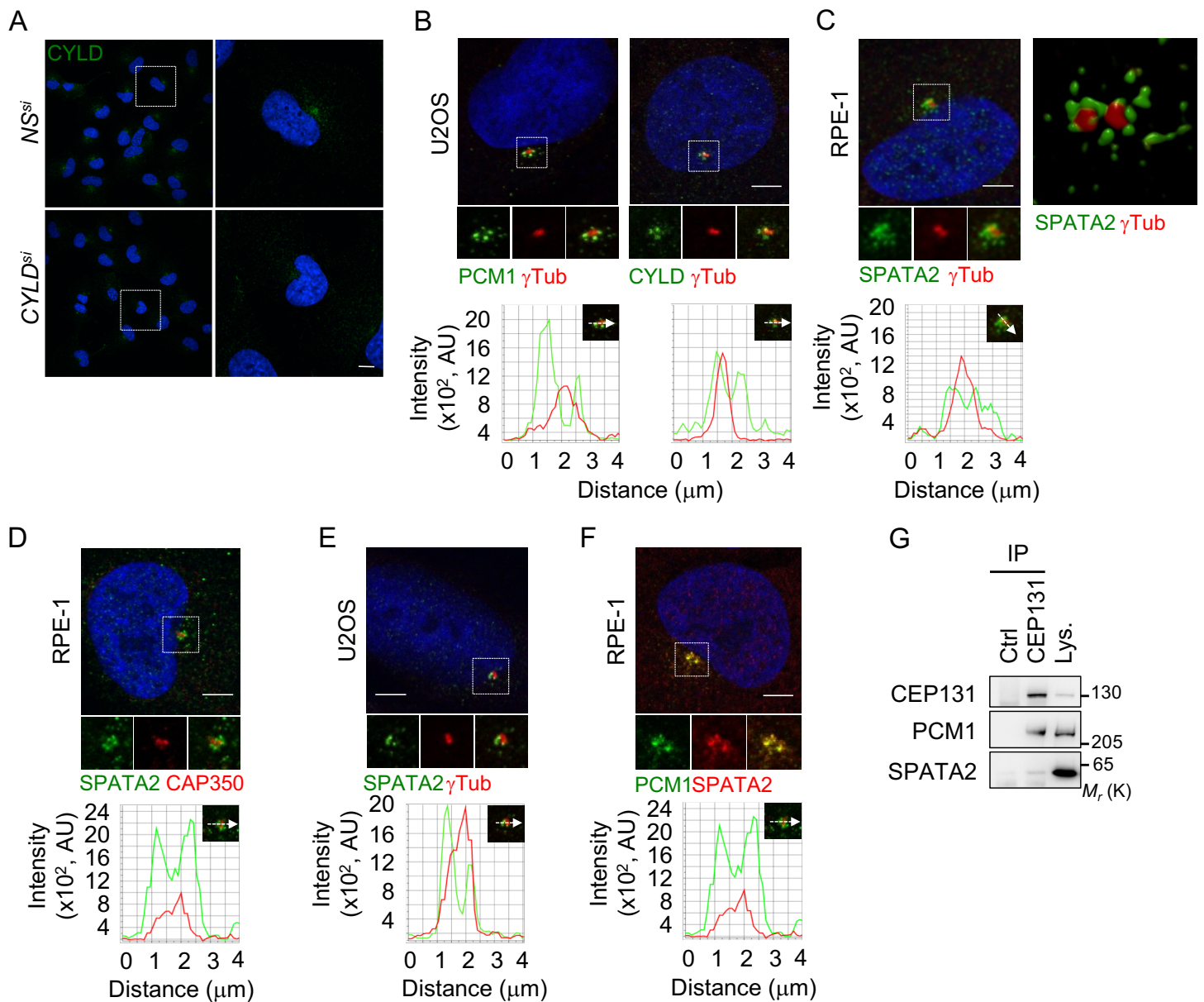


**Figure S2. CYLD is a Component of Centriolar Satellites, Related to Figure 2.**

**A**, Confocal images of RPE-1 cells transfected with siRNA for CYLD or scramble non-specific (NS) siRNA for 48 hours, fixed and immunostained as indicated. Nuclei were counterstained with 4',6-diamidino-2-phenylindole (DAPI). Regions highlighted by white squares are shown under higher magnification in panels on the right. Scale bar, 5  $\mu$ m. **B**, The localization of PCM1, CYLD and  $\gamma$ Tubulin ( $\gamma$ Tub) was analyzed by confocal microscopy in U2OS cells. Regions highlighted by white squares are shown under higher magnification in panels on the bottom. Scale bar, 5  $\mu$ m. Quantification of staining intensity alongside white arrow is shown. AU, arbitrary units. **C-E**, Confocal microscopic analysis of RPE-1 (**C** and **D**) and U2OS (**E**) cells showing the localization of the centrosome resident proteins  $\gamma$ Tubulin ( $\gamma$ Tub) or CAP350 together with SPATA2. Regions highlighted by white squares are shown under higher magnification in panels on the bottom. In (**C**), staining was analyzed by Structure Illumination microscopy (SIM). Nuclei were counterstained with DAPI. Scale bar, 5  $\mu$ m. Quantification of staining intensity alongside white arrow is shown. **F**, Analysis of ectopically expressed PCM1-GFP and SPATA2 by confocal microscopy in RPE-1 cells. Regions highlighted by white squares are shown under higher magnification in panels on the bottom. Scale bar, 5  $\mu$ m. Quantification of staining intensity alongside white arrow is shown. **G**, Cell lysates (Lys.) from RPE-1 cells were subjected to immunoprecipitations (IP) with antibodies against the indicated proteins, and samples were then analyzed by immunoblotting as indicated. Ctrl, non relevant isotype matched antibodies. Molecular weight markers are shown.

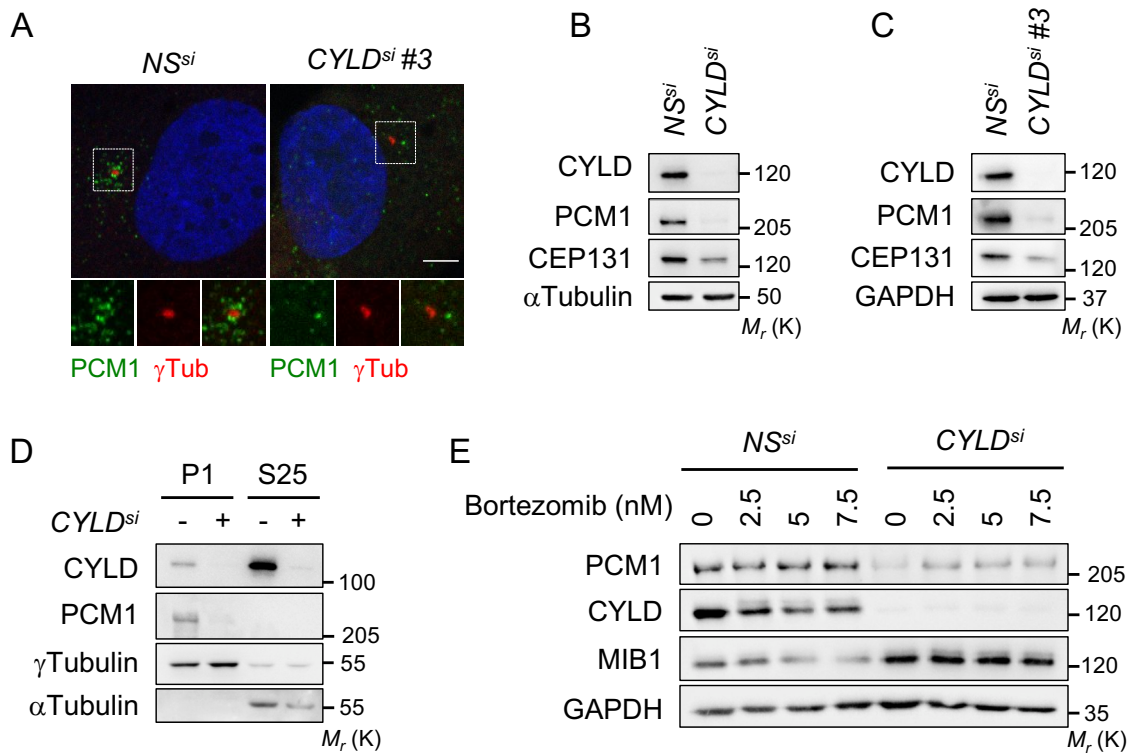


**Figure S3. CYLD controls the Proteostasis of Centriolar Satellites, Related to Figure 3.**

**A**, Confocal micrographs of RPE-1 cells transfected with siRNA for CYLD (sequence #3) or scramble non-specific (NS) siRNA for 48 hours, fixed and immunostained with antibodies to PCM1 and  $\gamma$ Tubulin ( $\gamma$ Tub). Nuclei were counterstained with 4',6-diamidino-2-phenylindole (DAPI). Regions highlighted by white squares are shown under higher magnification in panels on the bottom. **B**, HeLa cells were transfected with siRNA for CYLD or NS siRNA for 48 hours. Cell lysates were prepared and analyzed by immunoblotting with antibodies specific to the indicated proteins. Molecular weight markers are shown. **C**, RPE-1 cells were transfected with siRNA for CYLD (sequence #3) or NS siRNA for 48 hours. Cell lysates were prepared and analyzed by immunoblotting with antibodies specific to the indicated proteins. **D**, Fractions enriched with centriolar satellites and centrosomes (P1) or with cytosol (S25) from NS- and CYLD-silenced RPE-1 cells were analyzed by immunoblotting. **E**, RPE-1 cells as in (D) were treated 24 hours with the indicated concentrations of Bortezomib. Cell lysates were analyzed by immunoblotting as described in (B).

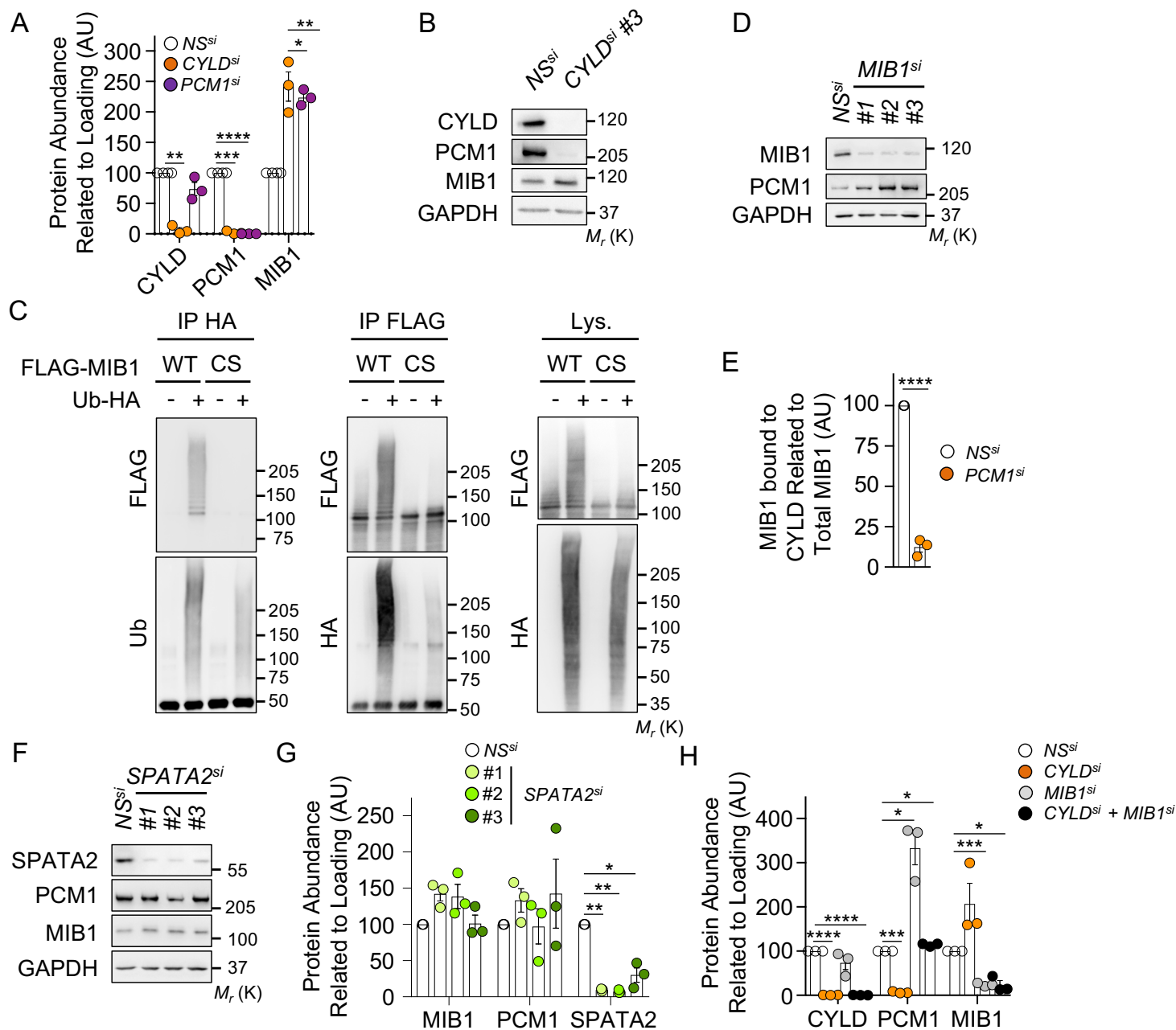


**Figure S4. CYLD prevents the E3 ligase MIB1 from dismantling Centriolar Satellites, Related to Figure 4.**

**A**, The intensities of the bands as in Fig. 4A were quantified, and the ratios of the intensities of the indicated bands normalized to those of GAPDH were calculated and are shown as means  $\pm$  SEM of three independent experiments. \* $P < 0.05$ ; \*\* $P < 0.01$ ; \*\*\* $P < 0.001$ ; \*\*\*\* $P < 0.0001$  (ANOVA). AU, arbitrary units. **B**, RPE-1 cells were transfected with siRNA for CYLD (sequence #3) or NS siRNA for 48 hours. Cell lysates were prepared and analyzed by immunoblotting with antibodies specific to the indicated proteins. **C**, HEK293T cells were transfected with plasmids encoding for FLAG-MIB1-WT or FLAG-MIB1-CS, or an empty vector and HA-tagged ubiquitin (Ub). Cell lysates (Lys.) were prepared and subjected to immunoprecipitation (IP) prior immunoblotting analysis with antibodies specific to the indicated proteins. Molecular weight markers are shown. **D**, RPE-1 cells were transfected for 48 hours with a non-specific (NS) siRNA or with three individual MIB1-specific siRNA. Cell lysates were analyzed by immunoblotting as indicated. **E**, The intensities of MIB1 bands bound to CYLD as in Fig. 4C were quantified, and the ratios of the intensities of the indicated bands normalized to those of MIB1 lysates were calculated and are shown as means  $\pm$  SEM of three independent experiments. \*\*\*\* $P < 0.0001$  (ANOVA). **F and G**, Lysates from RPE-1 cells transfected with NS siRNA or with three individual SPATA2-specific siRNA for 48 hours were subjected to immunoblotting with antibodies specific to the indicated proteins. The intensities of the bands as in (F) were quantified, and the ratios of the intensities of the indicated bands normalized to those of GAPDH were calculated (means  $\pm$  SEM of three independent experiments. \* $P < 0.05$ ; \*\* $P < 0.01$  (ANOVA)). **H**, The intensities of the bands as in Fig. 4I were analyzed as in (A).